Q. J. R. Meteorol. Soc. (1991), **117**, pp. 421–426 551.577.51:551.558.21(410.3)

Role of detailed wind–topography interaction in orographic rainfall

By P. ALPERT and H. SHAFIR

Department of Geophysics and Planetary Sciences, Raymond and Beverly Sackler Faculty of Exact Sciences, Tel Aviv University, Tel Aviv 69978, Israel

(Received 23 October 1989; revised 2 October 1990)

SUMMARY

A meso γ-scale ($\Delta x = 1$ km) model for orographic rainfall was used to investigate the dependence of orographic enhancement on wind speed and direction and on detailed topography. Applying the model to cases reported in south Wales, high sensitivity to wind direction and the corresponding upwind topographical cross-sections—factors neglected in some previous studies—was found. This suggests that studies of high-resolution orographical rainfall characteristics (such as orographic enhancement as function of wind speed) or model verification should account for detailed interaction of the wind vector with the high-resolution topography. Comparison with microphysical models illustrates that the effect of detailed wind–topography interaction is at least of similar magnitude to that due to microphysical processes.

1. INTRODUCTION

One of the most difficult problems in mountain meteorology is the accurate prediction/diagnosis of precipitation over complex topography. Theoretical studies by Collier (1975), Storebo (1976), Bader and Roach (1977, hereafter BR), Bell (1978), Carruthers and Choularton (1983, hereafter CC), Richard *et al.* (1987, hereafter RCMN), Richard and Chaumerliac (1989, hereafter RC), as well as others supported the seeder–feeder idea that was proposed by Bergeron (1965) and Browning (1980). However, these models and others have not compared the meso γ-scale ($\Delta x = 1$ km) geographical distribution of precipitation over complex topography with similar resolution in the observations. Alpert and Shafir (1989a, b, hereafter ASa, ASb) following Alpert (1986) illustrated the possibility of simulating high-resolution meso γ-scale rainfall fields over mountainous regions in Israel. They compared their results with observed rainfall distributions as derived from radar measurements by Rosenfeld (1986) and from raingauge data.

Hill *et al.* (1981, hereafter HBB), using both radar and raingauge rainfall observations for eight detailed case-studies over the Glamorgan Hills in south Wales, derived certain orographic rainfall characteristics. The HBB findings were subsequently used by some researchers to investigate orographic rainfall characteristics. These models assumed a constant topographical slope and wind direction. However, Hill and Browning (1981) and Hill (1983) have shown in a comprehensive observational study that the orographic rainfall distributions are highly sensitive to wind speed and in particular to the wind direction. Here, the AS model is applied to study the orographical rainfall enhancement features while the microphysical processes were not incorporated. The model simulations are described in section 2, section 3 discusses the results, and the conclusions are in section 4.

2. MODEL SIMULATIONS AND COMPARISON WITH OBSERVATIONS

The study domain is located over the Glamorgan Hills in south Wales. HBB investigated the dependence of orographic rainfall enhancement on low-level wind speed and on the background rainfall intensity, P_0. The rainfall rate at a coastal site—raingauge 4 in Fig. 1—was chosen as P_0 and was compared with that at a hilltop location determined by either raingauge 5 or 6, see HBB. In Table 1 the cases used for the HBB analysis are listed along with the model parameters discussed later.

Following ASa the precipitation at a point (x, y) whose altitude is given by $Z_s(x, y)$ is estimated by

$$P = \rho \varepsilon r\, e_s[\mathbf{V} \cdot \nabla Z_s + W_l]/(RT), \tag{1}$$

where P represents precipitation rate, $\mathbf{V}$ the mean horizontal velocity in the planetary boundary layer, W_l is the large scale (synoptic) vertical velocity contribution, $\varepsilon = 0.622$, $r = e_a/e_s$, e_a and e_s are the air vapour pressure and the saturated surface vapour pressure, respectively, R is the gas constant, ρ is an empirically determined factor representing 'precipitation efficiency', and the temperature, T, at the altitude Z_s is assumed to decrease with elevation by the observed lapse

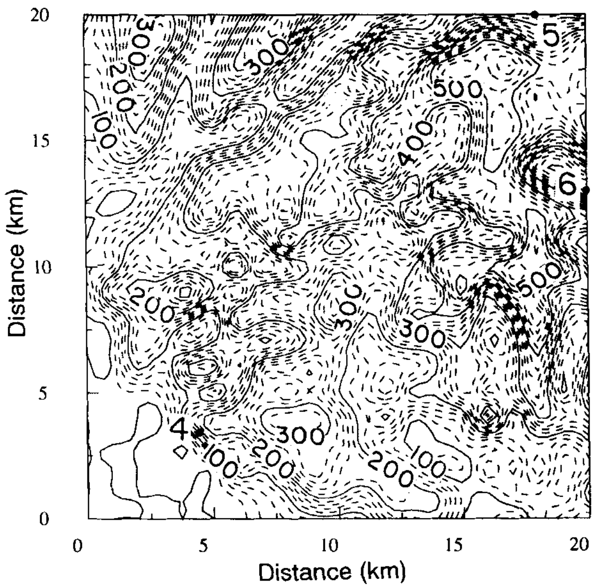

Figure 1. Detailed topography of the model domain for south Wales. Dashed topographic contours are at 20 m intervals and the solid lines are at 100 m intervals. The numbers indicate raingauges following HBB.

TABLE 1. INPUT PARAMETERS FOR THE MODEL IN THE VARIOUS EXPERIMENTS FOLLOWING HBB

Experiment No.	Wind vector at 600 m AMSL (deg/m s^{-1})	1000 mb temperature (K)	Lapse rate (K km^{-1})	Relative humidity (%)
1	230/30	283.5	4.5	90
2	220/26	282.5	5	93
3a	205/23	284	7.5	85
3b	230/26	284	7.5	85
4a	250/16	282	5.5	90
4b	240/22	282	5.5	90
4c	245/26	282	5.5	90
5	235/20	283	7	87
6a	220/19	279.5	5.5	92
6b	230/17	279.5	5.5	92
7a	200/15	284	4.5	87
7b	180/18	284	4.5	87
7c	260/21	284	4.5	87
8	260/14	283	7	80

rate, Γ; e_s is a function of T only and is determined by the Clausius–Clapeyron relation. For comparison with observations, it was shown to be useful to advect the precipitation downstream by the horizontal wind $\mathbf{V}$. Accordingly the precipitation became the normally weighted sum of the values upstream, see ASa. The wind vector of the 1000–900 mb layer was used to represent the mean boundary-layer velocity in the following experiments. The negative precipitation due to negative slopes is assumed to be zero, and in the present study W_l was put to zero since it was assumed that the value of P given by Eq. (1) corresponded to the enhancement of rainfall from coast to hills rather than to the total rainfall.

The present model has two parameters, i.e. the precipitation efficiency ρ and the advective time scale t (see ASa), that could be considered as tuning parameters. To eliminate an arbitrary choice of the two parameters, a procedure was developed to determine objectively their optimal values. This was done by performing a series of experiments in which ρ and t were gradually varied until a minimum root-mean-square error (RMSE) (as compared with the observations) was achieved. It should be stressed, however, that these parameters cannot affect the overall model performance except by a constant multiplication of all the results by the efficiency factor, and the smoothing through the advection.

Each of the aforementioned HBB cases was run with the corresponding input parameters (Table 1). The mean relative humidity (RH) in the lowest 1000 m as given by HBB is used for the fractional RH (r) in Eq. (1). Equation (1) was solved numerically over a 21×21 grid with an interval of $\Delta x = \Delta y = 1$ km. The topographic heights at each grid point were obtained directly from a 1:50000 map. In contrast to previous simulations of HBB cases by BR and RCMN who used a constant slope, here, the detailed topographic cross-sections, and wind speeds and directions, served as input in the model, see Fig. 1. Figure 2 shows the topographical cross-sections for the 14 HBB cases each in the reported upwind direction from the verifying raingauge, following the wind at 600 m above mean sea level (AMSL). The topography in Fig. 2 and in the simulations are

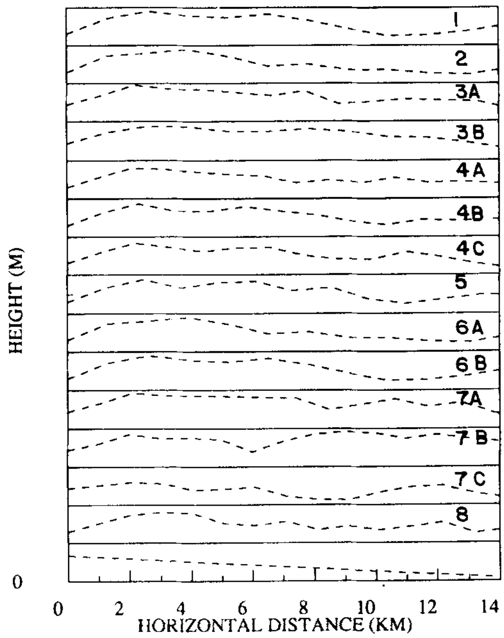

Figure 2. The 14 topographical cross-sections in the model simulations of HBB cases, based on a 1:50000 map of the Landranger series No. 170. The constant slope at the bottom is 1:40 as used by RCMN. Each rectangle height corresponds to 600 m.

without any smoothing. However, effective smoothing is introduced by the upwind difference scheme in calculating ∇Z_s. The term $\mathbf{V}\cdot\nabla Z_s$ is calculated by $(u\,\Delta Z_s/\Delta x + v\,\Delta Z_s/\Delta y)$. Hence, the slopes used for each grid point were obtained by differencing the two height values at a distance of 2 km ($2\Delta x$ or $2\Delta y$) upstream and at the pertinent point. The upwind trajectory was represented by the two grid points closest to it in each column, through simple distance interpolation, and the values of P for these points were weighted by the normal distribution function and then summed to give the model's estimate of enhanced precipitation.

Figures 3(a)–(c) show the model simulated against the observed rainfall enhancement for the 14 cases. The first experiment—verified in Fig. 3(a)—used our model with the realistic slopes from Fig. 2. Figure 3(b) presents RCMN verification while Fig. 3(c) is our model verification for a constant slope as used by RCMN. A comparison of Fig. 3(a) with Fig. 3(b) (i.e. our simulation with the realistic slopes with that with the full microphysics by RCMN) indicates that both models perform equally well*. It is interesting to note that the error signs for the two simulations are the same in most cases (except for experiments 3a and 3b) although the two model approaches differ considerably. Comparing the realistic slope simulations (Fig. 3(a)) with the constant slope ones

* The model overestimation of the rainfall for experiment 7c could be the result of very steep slopes found upwind (260°) from raingauge 5 right at the canal which extends south-west to the Swansea Bay (see Fig. 1).

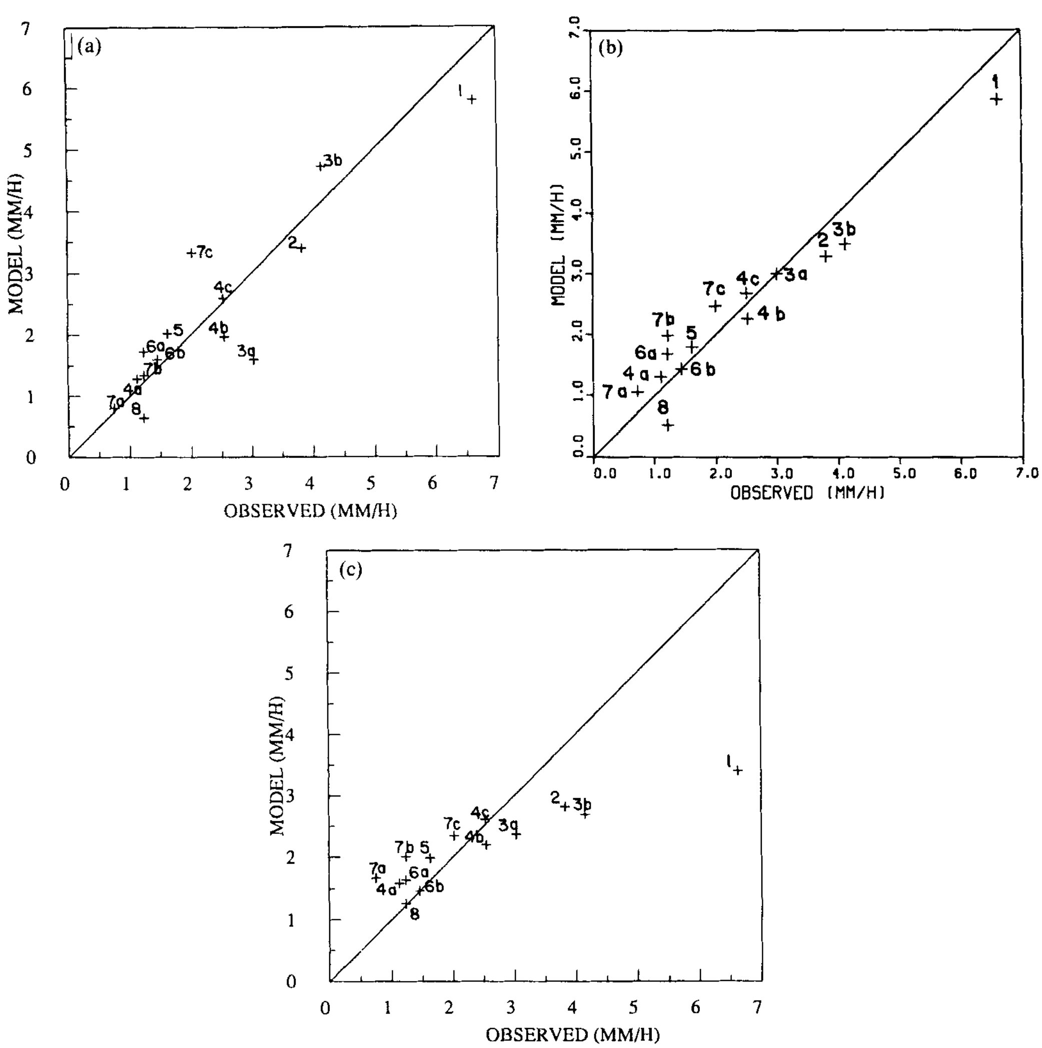

Figure 3. The model simulated against observed rainfall enhancement for the 14 HBB cases as follows: (a) present model with realistic slopes, (b) RCMN model, and (c) present model with a constant slope.

(Fig. 3(c)) shows a clear deterioration for the constant-slope simulations. The RMSE increases from 0.66 to 1.02 mm h^{-1} for the constant slope. The reduction in the rainfall for case 1 is explained by the exclusion of the sharp slopes found upwind (230°) from raingauge 6—See Fig. 1. Figure 2 does *not* show these steep slopes because they are only introduced through the numerical difference scheme which incorporates the neighbouring points upwind with the highly steep slopes. It should be mentioned that the aforementioned optimization method was applied in both experiments—realistic and constant slopes producing the same time scale of $t = 170$ s and about the same $\rho =$ 0.15–0.16.

In the more recent study of different microphysical parametrizations RC show (their Fig. 11) that by switching from one parametrization (Kessler 1969) to another (Berry and Reinhardt 1974), similar changes in the agreement with observations occur, i.e. RMSE changes from 1.2 to 0.6 mm h^{-1}. Hence, our comparison illustrates that the effects of detailed wind plus topography interaction could be at least of similar magnitude to that due to the microphysical processes.

3. Orographic enhancement dependence on wind and upwind rainfall

Hill *et al.* (1981) have constructed a curve representing the mean enhancement of the rainfall intensity from the Glamorgan coast (raingauge 4) to the Glamorgan Hills (raingauge 5 or 6) plotted as a function of the windspeed at 600 m AMSL. Subsequently, RCMN (Fig. 9) and RC used this curve to verify the microphysical processes in their models. To examine the effect of realistic wind and topography on the curve of orographic enhancement versus wind speed, we reran the model for various wind directions, Fig. 4. It is suggested that the HBB curve might result from a superposition of different wind directions and speeds. These curves are also strongly influenced by the choice of the hilltop raingauge (raingauge 5 or 6). For instance, compare curves (c) and (e) for raingauges 5 and 6 respectively. They are for the same wind direction but still differ considerably from each other.

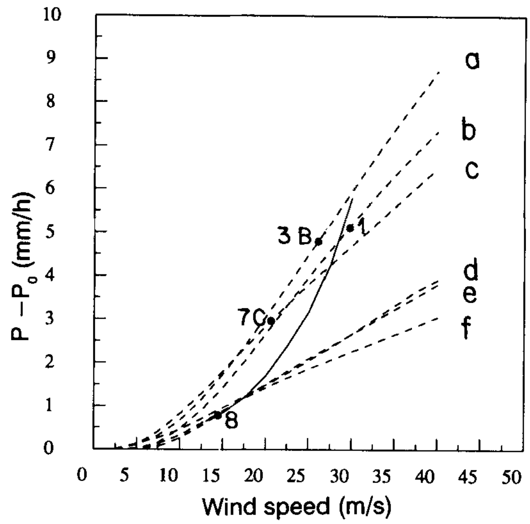

Figure 4. Model mean enhancement of the surface rainfall intensity from the Glamorgan coast to the Glamorgan Hills plotted as a function of the wind speed at 600 m AMSL. Solid line is the HBB curve. The additional curves are each for specific wind direction and hilltop raingauge (5 or 6) as follows: (a) 230° 5, (b) 230° 6, (c) 260° 5, (d) 180° 6, (e) 260° 6, (f) 180° 5. Results from some of the HBB cases are indicated.

Previous modelling encountered difficulties in obtaining large enhancements (~6 mm h^{-1}). RCMN have related this to the non-linear effects upon the vertical velocity, while CC have associated it with deep moist low-level jets. Figure 4 illustrates that such enhancements are readily obtained in a linear model and without jets.

HBB investigated the orographic enhancement (i.e. $P - P_0$) dependence on the background (coastal upwind) rainfall rate, and have constructed a functional relationship based upon the 14 aforementioned cases (HBB, Fig. 15). They found a strong dependence of enhancement on wind speed as well as a weak dependence on the upwind precipitation rate. The present model was rerun for the various wind directions reported in HBB cases except that the wind speed was varied until the same rainfall enhancement (i.e. 2 mm h^{-1}) was obtained. The corresponding range of wind speeds was found to be 17 to 29 m s^{-1} although all the other input parameters were kept constant. The large variability with wind direction and detailed topography puts into question the significance of drawing similar curves in the presence of strong wind changes.

4. Conclusions

The functional relationships suggested by HBB were re-examined by using a model which incorporated the detailed wind and topography upwind in each of the HBB cases. Our results were compared with the observations, and the model was found to perform equally well when compared with other models which include microphysical processes explicitly. Rerunning our simulations with a constant slope—as used by previous modellers—showed a significant deterioration in comparison with observations. Additionally, the curve describing the orographic enhancement dependence upon the low-level wind speed is shown to be strongly influenced by the different wind directions. It is suggested that the variability in the orographic rainfall enhancement due to the detailed topography may screen the weak dependence upon the seeding rate.

In summary, the sensitivity of orographic rainfall enhancement to accurate wind and topography upwind is probably larger than that assumed in previous studies. Hence, the curves proposed by HBB which neglect these effects may not be representative for the general behaviour of orographic enhancements.

ACKNOWLEDGEMENTS

Thanks to the Bi-National US–Israel Science Foundation for partly supporting H. Shafir through grant No. 8600230. Many thanks to Ms. Rachel Duani for typing the manuscript, Mr. A. Dvir for drafting some of the figures and D. Lawson for the topographical map.

REFERENCES

Alpert, P. 1986 Mesoscale indexing of the distribution of orographic precipitation over high mountains. *J. Climate Appl. Meteorol.*, **25**, 532–545

Alpert P. and Shafir, H. 1989a Meso γ-scale distribution of orographic precipitation: Numerical study and comparison with precipitation derived from radar measurements. *J. Appl. Meteorol.*, **28**, 1105–1117

1989b A physical model to complement rainfall normals over complex terrain. *J. Hydrol.*, **110**, 51–62

Bader, M. J. and Roach, W. T. 1977 Orographic rainfall in warm sectors of depressions. *Q. J. R. Meteorol. Soc.*, **103**, 269–280

Bell, R. S. 1978 The forecasting of orographically enhanced rainfall accumulations using 10-level model data. *Meteorol. Mag.*, **107**, 113–124

Barry, E. X. and Reinhardt, R. L. 1974 An analysis of cloud drop growth by collection: Part III Accretion and self-collection. *J. Atmos. Sci.*, **31**, 2118–2126

Bergeron, T. 1965 'On the low-level redistribution of atmospheric water caused by orography'. Suppl. Proc. Int. Conf. on Cloud Phys., Tokyo Meterol. Soc., May 1965, 96–100

Browning, K. A. 1980 Structure, mechanism and prediction of orographically enhanced rain in Britain. *Orographic Effects in Planetary Flows.* GARP Publication Series No. 23. Eds. R. Hide and P. W. White, 85–114

Carruthers, D. J. and Choularton, T. W. 1983 A model of the feeder–seeder mechanism of orographic rain including stratification and wind-drift effects. *Q. J. R. Meteorol. Soc.*, **109**, 575–588

Collier, C. G. 1975 A representation of the effects of topography on surface rainfall within moving baroclinic disturbances. *Q. J. R. Meteorol. Soc.*, **101**, 407–422

Hill, F. F. 1983 The use of average rainfall to derive estimates of orographic enhancement of frontal rain over England and Wales for different wind direction. *J. Climatol.*, **3**, 113–129

Hill, F. F. and Browning, K. A. 1981 'The use of climatological and synoptic data for forecasting orographic enhancement of rainfall.' *Proc. IAMAP Symp.*, Hamburg, 207–212

Hill, F. F., Browning, K. A. and Bader, M. J. 1981 Radar and raingauge observations of orographic rain over south Wales. *Q. J. R. Meteorol. Soc.*, **107**, 643–670

Kessler, E. 1969 On the distribution and continuity of water substance in atmospheric circulations. *Meteorol. Monog.*, **10**, No. 32, Am. Meteorol. Soc.

Richard, E. and Chaumerliac, N. 1989 Effects of different rain parameterizations on the simulation of mesoscale orographic precipitation. *J. Appl. Meteorol.*, **28**, 1197–1212

Richard, E., Chaumerliac, N., Mahfouf, J. F. and Nickerson, E. C. 1987 Numerical simulation of orographic enhancement of rain with mesoscale model. *J. Climate Appl. Meteorol.*, **26**, 661–669

Rosenfeld, D. 1986 'Dynamic characteristics of cumuliform cloud and cloud systems and their effect on the rainfall precipitated by them.' Ph.D. Thesis, The Hebrew University of Jerusalem

Storebo, P. B. 1976 Small scale topographic influence on precipitation. *Tellus*, **28**, 45–49